On analytical solutions to classes of definite integrals with products of Bessel functions of the first kind and their derivatives

L. A. Ambrosio,[1] G. Gouesbet,[2] and J. J. Wang[3]

[1)] *Department of Electrical and Computer Engineering. São Carlos School of Engineering, University of São Paulo. 400 Trabalhador são-carlense Ave. 13566-590, São Carlos, SP, Brazil.*

[2)] *CORIA-UMR 6614 - Normandie Université. CNRS-Université et INSA de Rouen. Campus Universitaire du Madrillet. 76800, Saint-Etienne du Rouvray, France.*

[3)] *School of Physics and Optoelectronic Engineering, Xidian University, 710071, Xi'an, China*

(*Electronic mail: leo@sc.usp.br)

(Dated: 12 February 2025)

In certain physical problems of light scattering, classes of integrals appear which involve particular products of Bessel functions of the first kind with complex argument and integer orders n and $n\pm1$ ($-\infty \leq n \leq \infty$), and also products of derivatives of such Bessel functions. Due to the lack of available analytical solutions in the literature, numerical calculations of these integrals have been recently carried out for the evaluation of photophoretic asymmetry factors (PAFs) in problems involving the illumination of lossy infinite cylinders, either in isolation or close to conducting corner spaces or planar boundaries, by plane waves or light-sheets. Here, we show that these integrals can actually be resolved analytically, therefore allowing for faster computation of physical quantities of interest in light scattering by small particles.

I. INTRODUCTION

In light scattering of arbitrary-shaped beams by micro-cylinder-shaped particles immersed in a simple and lossless gas or fluid, the incident, scattered and internal electromagnetic fields are usually expressed in terms of partial wave expansions using a cylindrical coordinate system[1–5]. The expanded internal fields are then subsequently incorporated into the formulas for the (radiant-absorption) heat generation function, Q[6–11], which in turn embodies all the necessary electromagnetic information regarding the calculation of photophoretic optical forces through the photophoretic asymmetry factors (PAFs). An accurate evaluation of the PAFs constitutes one of the first steps towards the determination of photophoretic forces, which are optical forces of thermal origin related to the light scattering and subsequent unbalanced heat absorption on the surface of the scatterer[12–22].

In recent investigations [see, e.g., Eqs. (30)-(33) of Ref.[23], Eqs. (16)-(19) of Ref.[24] and Eqs. (17)-(20) of Ref.[25]], Mitri has developed a semi-analytical method which provides reliable information on the longitudinal (L-) and transverse (T-) PAFs, either for cylinders in isolation or close to corner spaces[25] and planar boundaries[24], or even for aggregates of infinite cylinders[23]. The expansion coefficients for the internal fields are found from boundary conditions and, in all physical configurations, it can be noticed that, neglecting irrelevant multiplicative factors, constants and expansion coefficients which are of no interest here, the formulas for the L- and T-PAFs become proportional to the following integrals, which can be compactly represented as:

$$\mathcal{I}_1^+ = \int_0^1 \xi^2 J_n(m_c ka\xi) J_{n+1}(m_c^* ka\xi) d\xi, \tag{1}$$

$$\mathcal{I}_1^- = \int_0^1 \xi^2 J_n(m_c ka\xi) J_{n-1}(m_c^* ka\xi) d\xi, \tag{2}$$

and

$$\mathcal{I}_2^+ = \int_0^1 \left[\frac{n(n+1)}{|m_c|^2 (ka)^2} J_n(m_c ka\xi) J_{n+1}(m_c^* ka\xi) + \xi^2 J_n'(m_c ka\xi) J_{n+1}'(m_c^* ka\xi) \right] d\xi, \tag{3}$$

$$\mathcal{I}_2^- = \int_0^1 \left[\frac{n(n-1)}{|m_c|^2 (ka)^2} J_n(m_c ka\xi) J_{n-1}(m_c^* ka\xi) + \xi^2 J_n'(m_c ka\xi) J_{n-1}'(m_c^* ka\xi) \right] d\xi. \tag{4}$$

In Eqs. (1)-(4), n ($-\infty \leq n \leq \infty$) is an integer, m_c is the complex relative refractive index of the homogeneous cylinder with respect to the host fluid (gas or liquid) in which it is immersed, $k = 2\pi/\lambda$ is the wave number in the external lossless medium (λ is the wavelength) and a is the radius of the infinite cylinder. The asterisk denotes complex conjugation, and $J_\nu(z)$ are Bessel functions of the first kind, with a prime denoting differentiation with respect to the argument.

In this paper, we show that analytical solutions can be found for Eqs. (1)-(4), thus transforming semi-analytical calculations of L- and T-PAFs into pure analytical methods. In doing so, we shall make use of known solutions to particular integrals, Bessel's differential equation, integration by parts and

recurrence relations for Bessel functions. To the best of the authors' knowledge, the procedure here outlined cannot be found anywhere in the literature, nor any analytical solution to Eqs. (1)-(4) has been presented elsewhere.

We organize this paper as follows. In Sec. II we derive the solutions to Eqs. (1)-(4). Then, in Sec. III we provide quantitative information on the reduced computational burden offered by the present approach, as compared with the semi-analytical methods currently available. Finally, our conclusions are presented in Sec. IV.

II. GENERAL ANALYTICAL SOLUTIONS TO EQs. (1)-(4)

Let us rewrite Eqs. (1)-(4) in terms of a new variable $\rho = x\xi$, where $x = ka$ is the size parameter of the scatterer. For simplicity, we shall henceforth write $m_c = M$. Then, noticing that the complex conjugation can be placed outside the argument and applied directly to the Bessel functions and their derivatives themselves, we have, instead of Eqs. (1) and (2), the compact form:

$$g_1^{\pm} = \frac{1}{x^3}\int_0^x \rho^2 J_n(M\rho)J_{n\pm1}^*(M\rho)d\rho \tag{5}$$

and similarly, for Eqs. (3) and (4),

$$\begin{aligned} g_2^{\pm} =& \frac{1}{x^3}\int_0^x \left[\frac{n(n\pm1)}{|M|^2}J_n(M\rho)J_{n\pm1}^*(M\rho)\right. \\ &\left. + \rho^2 J_n'(M\rho)J_{n\pm1}'^*(M\rho)\right]d\rho. \end{aligned} \tag{6}$$

A. Analytical solution for Eq. (5)

To derive an analytic solution for Eq. (5), we start with a similar integral, which is valid for arbitrary real (not necessarily integer) order v:

$$\frac{1}{x^3}\int_0^x \rho^2 J_v(M\rho)J_{v\pm1}^*(M\rho)d\rho, \tag{7}$$

and make use of the following recurrence relations [see Eqs. (14.7) and (14.8), page 646 of Ref.[26], with comments in page 653 for non-integer order]:

$$J_{v\mp1}(M\rho) = \frac{v}{M\rho}J_v(M\rho) \pm J_v'(M\rho) \tag{8}$$

Substituting the complex conjugate of Eq. (8) in Eq. (7) for $J_{v\pm1}^*(M\rho)$, one then finds that

$$\begin{aligned} \frac{1}{x^3}\int_0^x \rho^2 J_v(M\rho)J_{v\pm1}^*(M\rho)d\rho =& \\ \frac{1}{x^3}\frac{v}{M^*}\int_0^x \rho|J_v(M\rho)|^2 d\rho& \\ \mp\frac{1}{x^3}\int_0^x \rho^2 J_v(M\rho)J_v'^*(M\rho)d\rho& \end{aligned} \tag{9}$$

The first integral in the r.h.s. of Eq. (9) can be resolved by introducing the following indefinite integral [see item 5.54, page 639 of Ref.[27], or Eq. (8), Sec. 5.11 of Ref.[28]]:

$$\int zJ_v(\alpha z)J_v(\beta z)dz = \frac{\alpha z J_{v+1}(\alpha z)J_v(\beta z) - \beta z J_v(\alpha z)J_{v+1}(\beta z)}{\alpha^2-\beta^2} \tag{10}$$

which, for integration from 0 to x and after setting $\alpha = M$, $\beta = M^*$ and $z = \rho$, can be recast under the form

$$\overline{R_v} \equiv \int_0^x \rho|J_v(M\rho)|^2 d\rho = \frac{\mathrm{Im}\left[MxJ_{v+1}(Mx)J_v^*(Mx)\right]}{\mathrm{Im}(M^2)}, \tag{11}$$

so that the first integral in the r.h.s. of Eq. (9) has been found.

For the last integral of Eq. (9), one can have recourse to Ref.[6], [see Eqs. (60) and (61) of the aforementioned reference, which also hold for arbitrary real order v]:

$$\begin{aligned} S_v \equiv& \int_0^x \rho\psi_v^*(M\rho)\psi_v'(M\rho)d\rho = \\ &-\frac{i}{2\,\mathrm{Im}(M^2)}\left\{x\left[M|\psi_v(Mx)|^2 + M^*|\psi_{v+1}(Mx)|^2\right]\right. \\ &-\frac{\pi|M|}{2}\left[\left(M + 2(v+1)\frac{\mathrm{Re}(M^2)}{M}\right)\overline{R_{v+1/2}}\right. \\ &\left.\left. + (2v+1)M^*\overline{R_{v+3/2}}\right]\right\}, \end{aligned} \tag{12}$$

where $\psi_v(z) = (\pi z/2)^{1/2}J_{v+1/2}(z)$ are Ricatti-Bessel functions.

After some straightforward algebra, the integral of Eq. (12) can be recast in terms only of Bessel functions and their derivatives:

$$\begin{aligned} S_v =& \frac{\pi|M|}{2}\frac{1}{2M}\overline{R_{v+1/2}} \\ &+ \frac{\pi|M|}{2}\int_0^x \rho^2 J_{v+1/2}^*(M\rho)J_{v+1/2}'(M\rho)d\rho \end{aligned} \tag{13}$$

which is equal to

$$
\begin{aligned}
S_v =& -\frac{i}{2\,\mathrm{Im}(M^2)}\frac{\pi x^2|M|}{2} \\
&\times\left\{M\left|J_{v+1/2}(Mx)\right|^2+M^*\left|J_{v+3/2}(Mx)\right|^2\right. \\
&-\frac{1}{x^2}\left(M+2(v+1)\frac{\mathrm{Re}(M^2)}{M}\right)\int_0^x\rho\left|J_{v+1/2}(M\rho)\right|^2 d\rho \\
&\left.+\frac{2v+1}{x^2}M^*\int_0^x\rho\left|J_{v+3/2}(M\rho)\right|^2 d\rho\right\}
\end{aligned}
\tag{14}
$$

From Eqs. (13) and (14), but with the substitution $v\to v-1/2$, it can be shown that

$$
\begin{aligned}
\int_0^x\rho^2 J_v^*(M\rho)J_v'(M\rho)d\rho &= \frac{2}{\pi|M|}S_{v-1/2}-\frac{1}{2M}\overline{R_v} \\
=&-\frac{i}{2\,\mathrm{Im}(M^2)}\left\{x^2\left[M|J_v(Mx)|^2+M^*|J_{v+1}(Mx)|^2\right]\right. \\
&\left.-\left[M+2\left(v+\frac{1}{2}\right)\frac{\mathrm{Re}(M^2)}{M}\right]\overline{R_v}+2vM^*\overline{R_{v+1}}\right\} \\
&-\frac{1}{2M}\overline{R_v}.
\end{aligned}
\tag{15}
$$

The terms proportional to $\overline{R_v}$ in Eq. (15) can be merged as follows:

$$
\begin{aligned}
&\frac{i}{2\,\mathrm{Im}(M^2)}\left[M+2\left(v+\frac{1}{2}\right)\frac{\mathrm{Re}(M^2)}{M}\right]\overline{R_v}-\frac{1}{2M}\overline{R_v} \\
&\quad=\frac{i}{2\,\mathrm{Im}(M^2)}\left[M+2\left(v+\frac{1}{2}\right)\frac{\mathrm{Re}(M^2)}{M}\right. \\
&\qquad\left.-\frac{1}{2M}\frac{2\,\mathrm{Im}(M^2)}{i}\right]\overline{R_v} \\
&\quad=\frac{i}{2\,\mathrm{Im}(M^2)}\left[\left(M+\frac{\mathrm{Re}(M^2)}{M}-\frac{1}{2M}\frac{2\,\mathrm{Im}(M^2)}{i}\right)\right. \\
&\qquad\left.+2v\frac{\mathrm{Re}(M^2)}{M}\right]\overline{R_v} \\
&\quad=\frac{i}{2\,\mathrm{Im}(M^2)}\left(2M+2v\frac{\mathrm{Re}(M^2)}{M}\right)\overline{R_v}
\end{aligned}
\tag{16}
$$

where, in passing from the second to the third identity in Eq. (16) we use the fact that $\mathrm{Re}(M^2)=[M^2+(M^2)^*]/2$ and $\mathrm{Im}(M^2)=[M^2-(M^2)^*]/2i$ to further simplify the terms under parenthesis.

After substitution of Eq. (16) in Eq. (15), one then gets

$$
\int_0^x\rho^2 J_v(M\rho)J_v'^*(M\rho)d\rho=(\overline{S_v})^* \tag{17}
$$

where

$$
\begin{aligned}
\overline{S_v} =& -\frac{i}{2\,\mathrm{Im}(M^2)}\left\{x^2\left[M|J_v(Mx)|^2+M^*|J_{v+1}(Mx)|^2\right]\right. \\
&\left.-2\left(M+v\frac{\mathrm{Re}(M^2)}{M}\right)\overline{R_v}+2vM^*\overline{R_{v+1}}\right\}
\end{aligned}
\tag{18}
$$

From Eqs. (9) and (11), together with the results found in Eqs. (15)-(18), we next impose $v=n$, where n is an integer, to finally conclude that

$$
\begin{aligned}
\frac{1}{x^3}\int_0^x\rho^2 J_n(M\rho)J_{n\pm1}^*(M\rho)d\rho =& \frac{1}{x^3}\left[\frac{n}{M^*}\overline{R_n}\mp(\overline{S_n})^*\right] \\
=& \mathcal{J}_1^{\pm},
\end{aligned}
\tag{19}
$$

in which $(\overline{S_n})^*$ is given by the complex conjugate of Eq. (18) and $\overline{R_n}$ by Eq. (11), both of which with $v=n$.

Equation (19) is the analytical solution we seek for Eq. (1) [or, equivalently, Eq. (5)].

B. Analytical solution for Eq. (6)

To analytically solve Eq. (6) for $\mathcal{J}_2^{\pm}$, we use Eq. (8) with $v=n$ an integer, together with the following recurrence relations which can also be derived from this equation:

$$
J_{n\pm1}'^*(M\rho)=\pm J_n^*(M\rho)\mp\frac{n\pm1}{M^*\rho}J_{n\pm1}^*(M\rho). \tag{20}
$$

From Eqs. (8) and (20), the term $\rho^2 J_n'(M\rho)J_{n\pm1}'^*(M\rho)$ in Eq. (6) can be put in the form:

$$
\begin{aligned}
\rho^2 J_n'(M\rho)J_{n\pm1}'^*(M\rho) =& \rho^2\left(\mp J_{n\pm1}(M\rho)\pm\frac{n}{M\rho}J_n(M\rho)\right) \\
&\times\left(\pm J_n^*(M\rho)\mp\frac{n\pm1}{M^*\rho}J_{n\pm1}^*(M\rho)\right) \\
=&-\rho^2 J_n^*(M\rho)J_{n\pm1}(M\rho)+\frac{n\pm1}{M^*}\rho J_{n\pm1}(M\rho)J_{n\pm1}^*(M\rho) \\
&+\frac{n}{M}\rho J_n(M\rho)J_n^*(M\rho)-\frac{n(n\pm1)}{|M|^2}J_n(M\rho)J_{n\pm1}^*(M\rho)
\end{aligned}
\tag{21}
$$

Substituting Eq. (21) into Eq. (6), one notices that the first term in the integrand of Eq. (6) is cancelled out by the last term of Eq. (21). In addition, the integral associated with the first term in the r.h.s. of the last identity of Eq. (21) is, except

for a sign change, nothing but $(\mathcal{I}_1^{\pm})^*$, which has been determined in the previous subsection and is given by the complex conjugate of Eq. (19). As for the second and third terms in the r.h.s. of Eq. (21), they are directly proportional to $\overline{R_{n\pm1}}$ and $\overline{R_n}$, respectively. Gathering it all, one can re-express Eq. (6) as

$$\frac{1}{x^3}\int_0^x \left[\frac{n(n\pm1)}{|M|^2}J_n(M\rho)J^*_{n\pm1}(M\rho) + \rho^2 J'_n(M\rho)J'^*_{n\pm1}(M\rho)\right]d\rho = -\frac{1}{x^3}\left(\frac{n}{M}\overline{R_n}\mp\overline{S_n}\right) + \frac{1}{x^3}\frac{n\pm1}{M^*}\overline{R_{n\pm1}} + \frac{1}{x^3}\frac{n}{M}\overline{R_n}. \quad (22)$$

After simplification, Eq. (22) can be written as

$$\frac{1}{x^3}\int_0^x \left[\frac{n(n\pm1)}{|M|^2}J_n(M\rho)J^*_{n\pm1}(M\rho) + \rho^2 J'_n(M\rho)J'^*_{n\pm1}(M\rho)\right]d\rho = \frac{1}{x^3}\left(\frac{n\pm1}{M^*}\overline{R_{n\pm1}}\pm\overline{S_n}\right), \quad (23)$$

or, equivalently, as

$$\mathcal{I}_2^{\pm} = \frac{1}{x^3}\left(\frac{n\pm1}{M^*}\overline{R_{n\pm1}}\pm\overline{S_n}\right), \quad (24)$$

Equation (23) or, alternatively, Eq. (24), is the result we seek for the integral given in Eq. (6).

III. NUMERICAL AND COMPUTATIONAL CONSIDERATIONS

In order to establish the correctness of Eqs. (19) and (24), we have developed a code using the software *Wolfram Mathematica 12.1 Student Edition*. The code was then run on a personal computer [Intel(R) Core(TM) i7-3630QM CPU @ 2.40GHz, 16.0 GB], and both the elapsed times (E.T.) and calculated values (C.V.) have been saved.

Table I presents data for $\mathcal{I}_1^{\pm}$. Numerical calculations of Eq. (5) are represented by $\mathcal{I}_{1,num}^{\pm}$, while the corresponding analytical formulas [Eq. (19)] are represented by $\mathcal{I}_{1,ana}^{\pm}$. Table II shows similar results, but now for $\mathcal{I}_2^{\pm}$. Since we want to have an accurate comparison between Eqs. (1)-(4) and their analytical formulas given by Eqs. (19) and (24), in all numerical simulations we use a command which tries to evaluate the integral exactly (function "Integrate[$f(\rho)$,{ρ,ρ_{min},ρ_{max}}]", where $\rho_{min}=0$ and $\rho_{max}=x$) before attempting at any numerical approximation scheme (for instance, use of the function "NIntegrate[$f(\rho)$,{ρ,ρ_{min},ρ_{max}}]", see Wolfram Mathematica documentation[29]). Although computed values are shown with six significant digits, agreement has been checked and verified up to the 50^{th} significant digit.

Besides assuring the correctness of our analytical formulas, Tables I and II also reveals that the introduction of analytical formulas significantly reduce computational burden, as expected. To better appreciate the impact of such a reduction in an actual physical situation, let us illustrate the calculation of the PAFs for an infinite dielectric cylinder illuminated by a plane wave, according to the geometry presented in Fig. 1 of Ref.[24]. In this particular scenario, the wave propagates along the x axis of a Cartesian coordinate system (x,y,z), the main axis of the cylinder coinciding with the z axis. Therefore, the T-PAF $J_{e,y}$, the y component of the PAF, is equal to zero. Assuming a time-harmonic convention $\exp(+i\omega t)$, where ω is the angular frequency of the incident wave, the L-PAF $J_{e,x}$ can be expressed, after some rearrangement of Eq. (16) of Ref.[24], as follows:

$$\mathcal{J}_{e,x} = -x\,\mathrm{Im}(\varepsilon_c)\,\mathrm{Re}\sum_{n=-\infty}^{+\infty}\Big\{b_n^{TE}C_n^{TE}\Big[b_{n-1}^{TE*}C_{n-1}^{TE*}\mathcal{I}_2^- + b_{n+1}^{TE*}C_{n+1}^{TE*}\mathcal{I}_2^+\Big] + b_n^{TM}C_n^{TM}\Big[b_{n-1}^{TM*}C_{n-1}^{TM*}\mathcal{I}_1^- + b_{n+1}^{TM*}C_{n+1}^{TM*}\mathcal{I}_1^+\Big]\Big\}. \quad (25)$$

In Eq. (25), ε_c is the relative permittivity of the cylinder, $x=ka$ is its size parameter, b_n^{TX} are expansion coefficients which fully describes the spatial contents of a particular wave field ($TX=TE$ or TM, TE standing for "Transverse Electric" and TM for "Transverse Magnetic") and C_n^{TX} are coefficients for internal fields which depend on M and x (the size parameter of the cylinder), being obtained from electromagnetic boundary conditions at the surface of the cylinder.

The coefficients for internal fields C_n^{TE} and C_n^{TM} can be written as[24,30,31]:

$$C_n^{TE} = \frac{J'_n(x)H_n^{(2)}(x) - J_n(x)[H_n^{(2)}(x)]'}{J'_n(Mx)H_n^{(2)}(x) - MJ_n(Mx)[H_n^{(2)}(x)]'} \quad (26)$$

and

$$C_n^{TM} = \frac{J_n(x)[H_n^{(2)}(x)]' - J'_n(x)H_n^{(2)}(x)}{J'_n(Mx)[H_n^{(2)}(x)]' - MJ'_n(Mx)H_n^{(2)}(x)}. \quad (27)$$

Notice that, because of the time-harmonic convention, in this paper C_n^{TE} and C_n^{TM} are expressed in terms of Hankel functions $H_n^{(2)}(.)$, and not of $H_n^{(1)}(.)$.

Table III shows $\mathcal{J}_{e,x}$ for several values of $x=ka$ between 1 and 20, together with the E.T. for the evaluation of Eq. (25) carried out either numerically ($J_{e,x}^{num}$) or from Eqs. (19) and (24) ($\mathcal{J}_{e,x}^{ana}$). A TE configuration has been chosen, such that $b_n^{TE}=(-i)^n$ and $b_n^{TM}=0$[24]. The infinite sum in Eq. (25) has been truncated in accordance with Wiscombe's criterium $n_{max}=\mathrm{round}[x+4.05x^{1/3}+2]$[32], and we have used the same values of M and ε_c as in Tables I and II. This particular choice

TABLE I. Calculated values (C.V.) and elapsed times (E.T.), in seconds, for $\mathcal{I}_1^{\pm}$, for several values of n. $\mathcal{I}_{1,num}^{\pm}$ represents $\mathcal{I}_1^{\pm}$ as calculated from Eq. (5), while $\mathcal{I}_{1,ana}^{\pm}$ represents $\mathcal{I}_1^{\pm}$ as calculated from the analytic expression provided by Eq. (19). The cylinder has $x = ka = 20$ and a relative permittivity $\varepsilon_c = 2.4635 - i0.1193$ ($M = \sqrt{\varepsilon_c} = 1.5700 - i3.7993 \times 10^{-2}$). The value for ε_c has been chosen in accordance with Fig. 2 of Ref.[24]. Numerical outputs have been calculated using the function "Integral[$f(\rho)$,{ρ,ρ_{min},ρ_{max}}]", see Ref.[29].

	$\mathcal{I}_1^+$			$\mathcal{I}_1^-$		
n	C.V.[a]	E.T. ($\mathcal{I}_{1,num}^+$)[b]	E.T. ($\mathcal{I}_{1,ana}^+$)[b]	C.V.[a]	E.T. ($\mathcal{I}_{1,num}^-$)[b]	E.T. ($\mathcal{I}_{1,ana}^-$)[b]
0	$2.32279 \times 10^{-4} + i6.41880 \times 10^{-3}$	2.52520	0.0198955	$-2.32279 \times 10^{-4} - i6.41880 \times 10^{-3}$	0.399476	0.0206048
1	$7.01146 \times 10^{-4} + i6.39622 \times 10^{-3}$	0.503545	0.0195711	$2.32279 \times 10^{-4} - i6.41880 \times 10^{-3}$	0.516400	0.0206423
5	$2.61274 \times 10^{-3} + i6.08718 \times 10^{-3}$	0.533446	0.0193255	$1.94754 \times 10^{-3} - i6.19753 \times 10^{-3}$	0.527844	0.0211438
10	$4.47236 \times 10^{-3} + i5.24450 \times 10^{-3}$	0.644501	0.0177169	$4.10511 \times 10^{-3} - i5.45207 \times 10^{-3}$	0.664070	0.0181969
20	$5.93117 \times 10^{-3} + i2.54320 \times 10^{-3}$	1.13520	0.0173345	$6.17290 \times 10^{-3} - i2.83611 \times 10^{-3}$	1.15912	0.0173816
50	$6.81364 \times 10^{-17} + i2.06099 \times 10^{-18}$	0.485938	0.0054033	$5.81286 \times 10^{-16} - i1.77766 \times 10^{-17}$	0.542316	0.0061767
100	$1.08548 \times 10^{-82} + i2.76075 \times 10^{-84}$	0.499713	0.0022628	$4.27407 \times 10^{-81} - i1.08817 \times 10^{-82}$	0.523574	0.0027728

[a] All values are presented with six significant digits.
[b] Elapsed time is limited down to the minimum time interval (in seconds) recorded on the computer system.

TABLE II. Calculated values (C.V.) and elapsed times (E.T.), in seconds, for $\mathcal{I}_2^{\pm}$, for several values of n. $\mathcal{I}_{2,num}^{\pm}$ represents $\mathcal{I}_2^{\pm}$ as calculated from Eq. (6), while $\mathcal{I}_{2,ana}^{\pm}$ represents $\mathcal{I}_2^{\pm}$ as calculated from the analytic expression provided by Eq. (24). The cylinder has the same values of x and M as in Table I. Numerical outputs have been calculated using the function "Integral[$f(\rho)$,{ρ,ρ_{min},ρ_{max}}]", see Ref.[29].

	$\mathcal{I}_2^+$			$\mathcal{I}_2^-$		
n	C.V.[a]	E.T. ($\mathcal{I}_{2,num}^+$)[b]	E.T. ($\mathcal{I}_{2,ana}^+$)[b]	C.V.[a]	E.T. ($\mathcal{I}_{2,num}^-$)[b]	E.T. ($\mathcal{I}_{2,ana}^-$)[b]
0	$2.34433 \times 10^{-4} + i6.40751 \times 10^{-3}$	2.10647	0.0268280	$-2.34433 \times 10^{-4} - i6.40751 \times 10^{-3}$	2.67518	0.0202969
1	$6.76092 \times 10^{-4} + i6.38548 \times 10^{-3}$	5.65676	0.0292484	$2.34433 \times 10^{-4} - i6.40751 \times 10^{-3}$	1.61558	0.0205657
5	$2.34062 \times 10^{-3} + i6.07766 \times 10^{-3}$	5.81103	0.0266828	$2.13682 \times 10^{-3} - i6.18601 \times 10^{-3}$	5.99656	0.0203182
10	$4.33344 \times 10^{-3} + i5.23897 \times 10^{-3}$	6.08995	0.0217748	$4.01613 \times 10^{-3} - i5.44103 \times 10^{-3}$	6.21083	0.0166023
20	$6.22479 \times 10^{-3} + i2.54195 \times 10^{-3}$	7.35369	0.0202804	$6.15429 \times 10^{-3} - i2.84151 \times 10^{-3}$	7.13465	0.0155233
50	$2.94449 \times 10^{-16} + i9.00225 \times 10^{-18}$	4.53538	0.0071048	$2.39392 \times 10^{-15} - i7.40589 \times 10^{-17}$	4.55446	0.0054060
100	$2.13839 \times 10^{-81} + i5.44429 \times 10^{-83}$	5.07520	0.0031795	$8.24579 \times 10^{-80} - i2.10162 \times 10^{-81}$	4.52853	0.0024835

[a] All values are presented with six significant digits.
[b] Elapsed time is limited down to the minimum time interval (in seconds) recorded on the computer system.

of M and x ensures that we are actually picking up specific values of $J_{e,x}$ associated with the curve $J_{e,x}^{TE}$, Fig. 2(a) of Ref.[24].

For comparison, the E. T. recorded for the analytical calculation ($\mathcal{J}_{e,x}^{ana}$) of such a curve with a list of 100 points was of 334.525 s, or 5.57541 min, while the numerical evaluation using the buit-in function "Integrate[$f(\rho)$,{ρ,ρ_{min},ρ_{max}}]" ($\mathcal{J}_{e,x}^{num}$) demanded more than 13 hours (or, precisely, 13.7177 hours). The use of a numerical approximation scheme can reduce this time reasonably. If we allow the software to automatically select the best integration method ($\mathcal{J}_{e,x}^{num}|_{best}$), the E.T. reduces to 1,287.16 s, or 21.4527 min, which is still at least three times longer than the E.T. observed when using Eqs. (19) and (24). Maximum percentage error observed remained below 10^{-9}%.

As for the numerical integration based on the trapezoidal rule with a sampling step $\delta q = 10^{-3}$ ($\mathcal{J}_{e,x}^{num}|_{trap}$), as adopted in Ref.[24], numerical integration converged too slow and the computation of the integrals demanded additional specifications of both the working precision (the number of digits d_p to be maintained for internal computations) and the number of effective digits of accuracy, d_a. For $d_p = d_a = 6$, results were generated after 18,347.1 s, or 5.09641 hours. However, noticeable errors as high as 140% have been observed in this case and for the particular choices of d_p and d_a. It has been observed that, although the slope of the generated curves do not differ significantly, as illustrated in Fig. 1(a), errors are

TABLE III. Calculated values (C.V.) and elapsed times (E.T.), in seconds, for the L-PAF $\mathcal{J}_{e,x}$ under TE configuration, for different values of $x = ka$. $\mathcal{J}_{e,x}^{num}$ represents $\mathcal{J}_{e,x}$ as calculated from numerical integration of Eq. (6), while $\mathcal{J}_{e,x}^{ana}$ represents $\mathcal{J}_{e,x}$ as calculated from the analytic expression provided by Eq. (24). The cylinder has the same values of M and ε_c as in Tables I and II.

	$\mathcal{J}_{e,x}$		
$x = ka$	C.V.[a]	E.T. ($\mathcal{J}_{e,x}^{num}$)[b]	E.T. ($\mathcal{J}_{e,x}^{ana}$)[b]
1	0.00188092	177.847	0.172748
5	0.0309144	298.054	0.393333
10	-0.0113271	649.477	1.69427
15	-0.0795463	780.537	4.39050
20	-0.138282	924.008	7.78548

[a] All values are presented with six significant digits.
[b] Elapsed time is limited down to the minimum time interval (in seconds) recorded on the computer system.

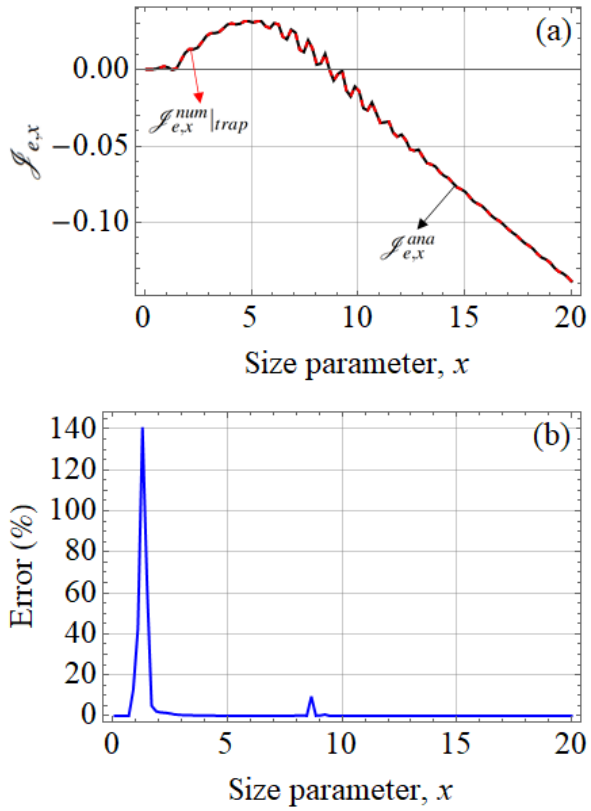

FIG. 1. (a) Reproduction of Fig. 2(a), curve "$J^{TE}_{e,x}$" of Ref.[24]. The red dashed curve corresponds to $\mathcal{J}_{e,x}|_{trap}$, while the black solic curve represents $\mathcal{J}^{ana}_{e,x}$. Curves have been computed with 100 points. Visually, they do not differ significantly. (b) Percentage error $100\left|(\mathcal{J}^{ana}_{e,x} - \mathcal{J}^{num}_{e,x}|_{trap})/\mathcal{J}^{ana}_{e,x}\right|$. Errors are larger for low values of the considered L-PAF.

high for low values of $J_{e,x}$ [Fig. 1(b)].

Since the integrals presented in Eqs. (1)-(4) are quite general, in the sense that they might be found in several other configurations beyond those presented in Refs.[23–25], we believe that the solutions here presented are of significant interest to the physics and engineering community in the fields of light scattering and photophoresis.

IV. CONCLUSIONS

In this paper we have derived analytical solutions to specific classes of definite integrals involving products between Bessel functions of the first kind with complex arguments and integer order n and $n\pm1$ and also between derivatives of such special function. In doing so, we have actually been able to pave the way for faster and accurate calculation of photophoretic asymmetry factors in light scattering by infinite cylinders. Since the same classes of integrals appear not only when dealing with isolated dielectric cylinders illuminated by plane waves, but with arbitrary refractive index cylinders or aggregates of them under illumination by arbitrary-shaped beams, the results here found might be of general application in several other investigations in the field of photophoresis involving infinite cylinders. Furthermore, we expect that extensions to products between Bessel functions of different kinds might be useful in problems which incorporate concentric and eccentric heterogeneous cylinders. This is currently in progress.

ACKNOWLEDGMENTS

L. A. Ambrosio acknowledges the partial finantial support of The Council for Scientific and Technological Development (CNPq) (426990/2018-8, 309201/2021-7) and of The São Paulo Research Foundation (FAPESP) (2020/05280-5).

DATA AVAILABILITY STATEMENT

The data that support the findings of this study are available from the corresponding author upon reasonable request.

REFERENCES

[1] G. Gouesbet and G. Gréhan, "Interaction Between Shaped Beams and an Infinite Cylinder, including a discussion of Gaussian beams," Particle & Particle Systems Characterization **11**, 299–308 (1994), https://onlinelibrary.wiley.com/doi/pdf/10.1002/ppsc.19940110405.
[2] G. Gouesbet, "Interaction between an infinite cylinder and an arbitrary-shaped beam," Appl. Opt. **36**, 4292–4304 (1997).
[3] K. F. Ren, G. Gréhan, and G. Gouesbet, "Scattering of a Gaussian beam by an infinite cylinder in the framework of generalized Lorenz–Mie theory: formulation and numerical results," J. Opt. Soc. Am. A **14**, 3014–3025 (1997).
[4] L. Mees, K. F. Ren, G. Gréhan, and G. Gouesbet, "Scattering of a Gaussian beam by an infinite cylinder with arbitrary location and arbitrary orientation: numerical results," Appl. Opt. **38**, 1867–1876 (1999).
[5] H. Zhang and Y. Han, "Scattering of shaped beam by an infinite cylinder of arbitrary orientation," J. Opt. Soc. Am. B **25**, 131–135 (2008).
[6] D. Mackowski, "Photophoresis of aerosol particles in the free molecular and slip-flow regimes," International Journal of Heat and Mass Transfer **32**, 843 – 854 (1989).
[7] S. A. Beresnev and L. B. Kochneva, "Radiation absorption asymmetry factor and photophoresis of aerosols," Atmospheric and Oceanic Optics **16**, 119–126 (2003).
[8] H. Horvath, "Photophoresis – a Forgotten Force ??" KONA Powder and Particle Journal **31**, 181–199 (2014).
[9] L. A. Ambrosio, "Photophoresis in the slip-flow and free molecular regimes for arbitrary-index particles," Journal of Quantitative Spectroscopy and Radiative Transfer **255**, 107276 (2020).
[10] L. A. Ambrosio, "Generalized Lorenz-Mie theory in the analysis of longitudinal photophoresis of arbitrary-index particles: On-axis axisymmetric beams of the first kind," Journal of Quantitative Spectroscopy and Radiative Transfer **275**, 107889 (2021).
[11] H. Wang, J. Wang, W. Dong, Y. Han, L. A. Ambrosio, and L. Liu, "Theoretical prediction of photophoretic force on a dielectric sphere illuminated by a circularly symmetric high-order Bessel beam: on-axis case," Opt. Express **29**, 26894–26908 (2021).
[12] M. Rosen and C. Orr, "The photophoretic force," Journal of Colloid Science **19**, 50 – 60 (1964).
[13] A. Akhtaruzzaman and S. Lin, "Photophoresis of absorbing particles," Journal of Colloid and Interface Science **61**, 170 – 182 (1977).
[14] Y. I. Yalamov, V. B. Kutukov, and E. R. Shchukin, "Motion of small aerosol particle in a light field," Journal of Engineering Physics **30**, 648 – 652 (1976).

[15] Y. Yalamov, V. Kutukov, and E. Shchukin, "Theory of the photophoretic motion of the large-size volatile aerosol particle," Journal of Colloid and Interface Science **57**, 564 – 571 (1976).
[16] L. D. Reed, "Low Knudsen number photophoresis," Journal of Aerosol Science **8**, 123 – 131 (1977).
[17] S. Arnold and M. Lewittes, "Size dependence of the photophoretic force," Journal of Applied Physics **53**, 5314–5319 (1982), https://doi.org/10.1063/1.331369.
[18] A. B. Pluchino, "Photophoretic force on particles for low knudsen number," Appl. Opt. **22**, 103–106 (1983).
[19] S. Arnold, A. B. Pluchino, and K. M. Leung, "Influence of surface-mode-enhanced local fields on photophoresis," Phys. Rev. A **29**, 654–660 (1984).
[20] W. M. Greene, R. E. Spjut, E. Bar-Ziv, A. F. Sarofim, and J. P. Longwell, "Photophoresis of irradiated spheres: absorption centers," J. Opt. Soc. Am. B **2**, 998–1004 (1985).
[21] W. M. Greene, R. E. Spjut, E. Bar-Ziv, J. P. Longwell, and A. F. Sarofim, "Photophoresis of irradiated spheres: evaluation of the complex index of refraction," Langmuir **1**, 361–365 (1985), https://doi.org/10.1021/la00063a017.
[22] V. Chernyak and S. Beresnev, "Photophoresis of aerosol particles," Journal of Aerosol Science **24**, 857 – 866 (1993).
[23] F. G. Mitri, "Photophoretic asymmetry factors for an absorptive dielectric cylinder near a reflecting planar boundary," J. Opt. Soc. Am. A **38**, 1901–1910 (2021).
[24] F. G. Mitri, "Longitudinal and transverse PAFs for an absorptive magneto-dielectric circular cylinder in light-sheets of arbitrary wavefronts and polarization," Appl. Opt. **60**, 7937–7944 (2021).
[25] F. G. Mitri, "Effect of a perfectly conducting corner space on the PAFs for an absorptive dielectric circular cylinder," J. Opt. Soc. Am. B **38**, 3910–3919 (2021).
[26] G. B. Arfken, H. J. Weber, and F. E. Harris, *Mathematical Methods for Physicists: A Comprehensive Guide* (Academic Press, Oxford, UK, 2012).
[27] I. S. Gradshteyn and I. M. Ryzhik, *Table of Integrals, Series and Products* (Academic Press, Burlington, MA, USA, 2007).
[28] G. N. Watson, *A Treatise on the Theory of Bessel Functions* (Cambridge University Press, Cambridge, UK, 1944).
[29] "Wolfram Language & System, Documentation Center," `https://reference.wolfram.com/language/`, accessed: 2022-01-18.
[30] H. C. van de Hulst, *Light scattering by small particles*, Dover books on physics (Dover, New York, NY, 1981).
[31] J. Stratton, *Electromagnetic theory* (McGraw-Hill, New York, 1941).
[32] W. J. Wiscombe, "Improved mie scattering algorithms," Appl. Opt. **19**, 1505–1509 (1980).